Iodine Recombination in Xenon Solvent: Clusters in the Gas to Liquid-like State Transition

M. Mirakhory, A. Majumdar, M. Ihme, A. C.T. van Duin

Abstract

Supercritical fluids have attracted significant attention as solvents for chemical reactions due to their unique properties, such as high diffusivity, low viscosity, and tunable solvation properties, which profoundly influence reaction kinetics. To study the effect of supercritical solvent on chemical reactivity and dynamics of reactions, one needs to understand the dynamics of clusters in supercritical fluid. Extensive experiments on the photodissociation and recombination of Iodine in supercritical fluids served as a model system for understanding these effects. Experimental studies followed by theoretical and computational investigations which mostly employed Monte Carlo or empirical molecular dynamics simulations. However, computational studies using non-reactive force fields and ab initio approaches present challenges in capturing reactive processes at larger scales within supercritical fluids. In this work, we developed the ReaxFF parameters by training against quantum mechanics data. ReaxFF reactive force field based molecular dynamics simulations were performed, studying the dynamics of a Xenon solvent and cage effect in different state conditions for Iodine recombination reaction. We show that the conditions near the critical point are the optimal conditions to study the cage effect. Our results indicate that increasing the size of the Xenon system beyond 1000 atoms does not change cluster size distribution significantly. We show that the average lifetime of Xenon clusters is in ranges between 5-11 picoseconds which allows Iodine atoms to undergo a geminate recombination within them. Our simulation results of Iodine recombination in Xenon solvent demonstrate the higher probability of Iodine molecule formation in the presence of Xenon clusters. Finally, we show that the supercritical condition exhibits the highest recombination rate for Iodine atoms, and increasing simulation timescales to up to 4 nanoseconds brings simulation results closer to experimental observations.

1. Introduction

Materials can be subjected to higher pressures and temperatures exceeding liquid-gas critical points. In this state, which is called the supercritical state, matter has both liquid-like solvent

properties as well as gas-like flow characteristics [1]. By varying the pressure, one can alter the density, as well as all equilibrium and transport properties that scale with the density, such as solvation power and viscosity [2], of a supercritical fluid across a wide range, ultimately resulting in the optimization of its solubility for a particular application. The solvation properties of supercritical fluids near its liquid-gas critical point are caused by the deformation of structure heterogeneities around the solute molecules which this structural heterogeneities are interpreted as clustering [3]. Supercritical fluids find applications as solvents in the processing of food and pharmaceuticals [4], as well as in propellants [5], [6].

Revealing the dynamics of elementary chemical reactions in solutions is essential since their rates are affected by both the solvent in which they take place and their kinetics. The transition between different solvent states, such as the transformation from a gas-like to a liquid-like state, has major impacts on chemical reactivity and kinetics due to the cage effects [7], [8] imposed by the solvent matrix. The cage effect, first proposed by Franck and Rabinowitch in 1934, states that solvents can constrain diffusion of initial atom pairs by geometric confinement, leading to recombination [9]. This phenomenon was first demonstrated by the photodissociation and recombination of Iodine in liquids. Noyes and coworkers [10], [11] found Iodine recombination as a function of solvent viscosity through their experiments. Subsequently, extensive research was conducted on the recombination of iodine atoms in fluids ranging in density from gases to liquids, as well as the solvent cage effect [12], [13], [14], [15], [16]. Elucidating the Iodine recombination dynamics was not feasible in a short time scale until Chuang at. al. [17] studied the process of predissociation and the recombination of Iodine atoms by picosecond laser excitation.

Iodine has been chosen as a prototype for various reasons. First is the availability of a considerable amount of information on many aspects of recombination of iodine atoms. Also, the simplicity of this diatomic molecule, besides the accessibility of I_2 photodissociation and recombination reactions experiments [13], [18] and sensitivity to solvent conditions, makes it an ideal option to provide a foundational understanding of chemical processes and reaction kinetics. Moreover, numerous experimental studies revealed the significant solubility of Xenon in liquid, near supercritical, and gaseous states for a wide variety of biological and organic molecules [19], [20]. Also, the complete optical transparency of Xenon in all of the UV and IR spectra region [21], [22] makes it a good candidate to study solute reactions [21], [22].

Experimental studies helped significantly in gaining detailed insight into these reactions and their kinetics; however, when dealing with complex systems with a large number of atoms and varying thermodynamic conditions, employing computational methods proves to be a more computationally efficient approach. Several studies have attempted to study the photodissociation and recombination of Iodine in different fluids using simulations and trajectory analysis [23], [24], [25], but no studies have been carried out to model Iodine recombination using reactive Molecular Dynamics (MD) simulation. Reactive force field simulations have been employed extensively to provide insight into chemical reactions [26], [27], [28], [29] with lower computational expenses and larger simulation scales while having the same order of accuracy as QM.

The unique properties and tunability of supercritical fluids, the importance of understanding reaction dynamics in solvents, and the advantages of reactive force fields all motivate the investigation of the physical chemistry of supercritical fluids as solvents and the cage effect on the dynamics of chemical reactions using reactive molecular dynamics simulations. In this study we develop and apply ReaxFF reactive force fields [30] to MD simulations to investigate the dynamics of the Xenon/Iodine system, the dynamics of solvent cage effect on the reaction kinetics of Iodine atoms and find a thermodynamic state condition for the Xenon system in which the highest Iodine recombination rate occurs.

2. Method

2.1.ReaxFF Method

Reactive force field based MD methods help to bridge the gap in simulation scale that separates quantum mechanics (QM) from empirical interatomic potentials that are based on classical approaches [30]. In this study, the ReaxFF MD method has been employed to understand the dynamic cluster behavior of the Xenon system for a wide range of thermodynamic conditions and its effect on the reaction kinetics of Iodine atoms.

ReaxFF is a general bond order-dependent force field that provides accurate descriptions of bond formation and bond breaking in a wide range of materials and chemical systems. Unlike traditional nonreactive force fields [31], [32], [33], ReaxFF distinguishes itself by dynamically determining

the connectivity via bond orders calculated from updated interatomic distances at each MD time step. The following energy expression is used in ReaxFF to determine the forces acting on each atom:

$$E_{sys} = E_{bond} + E_{over} + E_{under} + E_{lp} + E_{val} + E_{tor} + E_{vdWaals} + E_{coulomb} \quad \text{Equation 1}$$

Accounting for energy contributions related to the bond formation and dissociation, three-body valence angle strain, four-body torsional angle strain, overcoordination energy penalty, undercoordination stability, lone-pair energy, non-bonded van der Waals interactions, and Coulomb energies, respectively. ReaxFF is typically trained against quantum mechanics data, enabling ReaxFF to approach the accuracy of QM, covering significantly faster time scales than the QM method. Thus, this method can be used to simulate relatively large systems over long-time scales. ReaxFF can be used to study any novel system because its parameters are derived solely from QM, and it does not need any pre-defined reactive sites or reaction pathways.

2.2.Force Field Development

Similar to other empirical potentials [34], [35], [36], ReaxFF force fields are designed with system-specific considerations, and their parameters need to be tuned. These parameters are typically trained against experimental or QM-based data- most commonly Density Functional Theory (DFT) data. Before initiating MD simulations for large-scale systems to study Iodine recombination in supercritical Xenon solvent, we have developed a Xe/I reactive force field parameter set.

The DFT calculations were performed to obtain the potential energy surfaces for Xe/Xe, Xe/I, colinear Xe/I_2, and perpendicular Xe/I_2 atom pair interactions. For these simulations, we used the PBE exchange correlation functional [37] along with def2-TZVP basis set [38] and Grimme's D2 dispersion correction [39]. We also performed coupled cluster singles and doubles (CCSD) calculations to have a more accurate Xe/Xe potential energy surface using DGDZVP basis set [40,41]. To obtain the I/I potential energy surface we performed complete active space self-consistent field (CASSCF(6,8)) [42] simulations with the same basis set [43], since DFT underpredicted the potential energy well depth. All these quantum simulations were carried out using Gaussian 16 [44]. Moreover, DFT simulations were performed to train force field parameters

of the I-I-I angle. The GGA:PBE DFT functional [45] and TZP basis set were applied in DFT simulations using ADF/AMS software [46].

A successive single-parameter search optimization was performed to optimize the parameters and minimize the error following [47]:

$$Error = \sum_{i=1}^{n} \left[\frac{x_{i,QM} - x_{i,ReaxFF}}{\sigma}\right]^2$$

Equation **Error! No text of specified style in document.**

where σ represents the weight assigned to every data point based on its relative significance in the optimization process, and x is the data point in the training set, specifically energy in this study.

2.3.ReaxFF MD simulations Methodology

We employed our Xe/I force field to study the solvent clustering at different thermodynamic states and its effect on Iodine recombination. To validate the behavior of a Xenon system, initially, a system consisting of 11000 atoms was prepared in their energy-minimized structure in a periodic simulation box. Since different parameters affect the dynamics of solvent atoms and cluster size, the Xenon system was simulated with different sizes (500, 1000, 4000, and 10000 atoms) and thermodynamic states (liquid, supercritical, and gas state with temperature range of 202.6- 636.6K and pressure range of 58.98 -102 bar). NVT simulations were performed to study the behavior of solvent, where NVT indicates that the number of atoms (N), volume (V), and temperature (T) are kept constant during the simulations. The Berendsen thermostat with a temperature damping constant of 1000 fs is used to control the temperature. The timestep size in these simulations is 1 fs. Each simulation was performed for a total duration of 1 nanosecond (ns).

After studying the dynamics of solvent and examining the probability of cluster formations as well as their size and lifetime, Iodine atoms are added randomly to the system, and their recombination within Xenon clusters is investigated. The Iodine/Xenon atoms ratio in a system was chosen to be 1:40, taking into account both the efficacy of the cage effect and the potential for Iodine diffusion.

Initially, three types of ReaxFF_MD simulations were performed: 1)Single thermostat NVT, 2)Multiple thermostat NVT, and 3)NVE where NVE indicates that the number of atoms (N), volume (V), and Energy (E) are kept constant during the simulations. Unlike experiments where the temperature of the system remains constant without having active temperature control, the NVE ensemble in MD simulations with no control over temperature condition allows the temperature to fluctuate, potentially increase over time and failing to accurately mimic the supercritical conditions of a Xenon solvent. To achieve temperature control, we employed NVT ensemble in MD simulation. Furthermore, to ensure that the temperature control mechanism does not hinder the recombination of Iodine atoms, we performed multiple thermostat NVT simulations using a weaker thermostat specifically applied to the Iodine atoms. For single thermostat NVT simulation, the Berendsen thermostat with a temperature damping constant of 1000 fs is used to control the temperature, while in multiple thermostat NVT the temperature damping constant of Xenon atoms is 1000fs and the temperature damping constant of Iodine atoms is 1e6 fs. The timestep size in all these simulations is 0.25 fs. Each simulation was performed for a total duration of 1 nanosecond (ns).

To gain statistically meaningful results, an ensemble of ten simulation was performed that were initialized with random starting configurations, and the results were ensemble-averaged.

3. Results and discussion

3.1. Force field development

We have developed a Xe/I reactive force field parameter sets, encompassing the descriptions of Xe/Xe, I/I, Xe/I, as well as colinear and perpendicular Xe/I_2 pairs interactions during clustering and recombination. Using a single-parameter search optimization, these force field parameters were trained against the quantum chemical calculations data for reaction energies of atomic pair dissociations for smaller systems.

We carried out CASSCF calculations for I/I pair and DFT calculations for other pair interactions and parameterized the ReaxFF force field against this data. To accurately describe the non-covalent interactions (van der Waals) between Xenon pairs, we also add CCSD and Lennard Jones data to train our force field against it for an attractive part of the interaction. Figure 1 compares ReaxFF and QM results for each pair interaction.

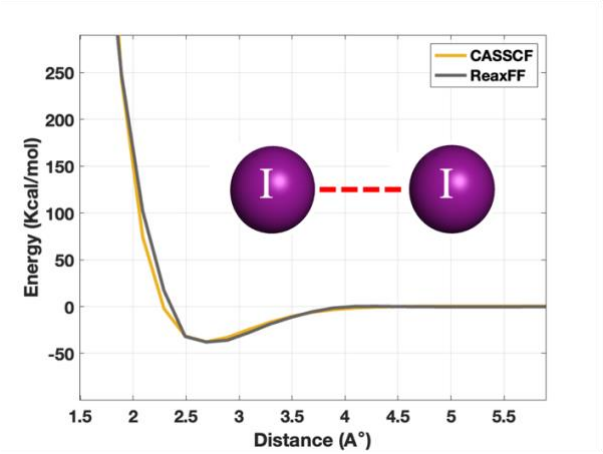

(a)I/I Pair interaction

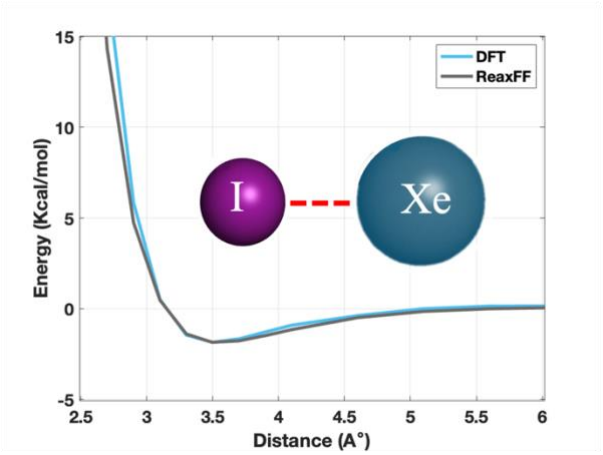

(b) I/Xe pair interaction

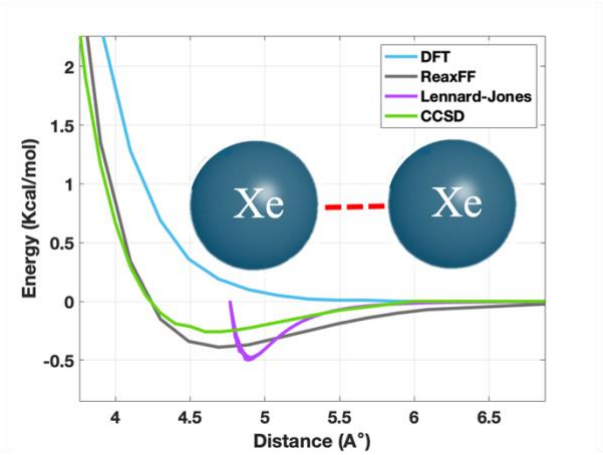

(c) Xe/Xe pair interaction.

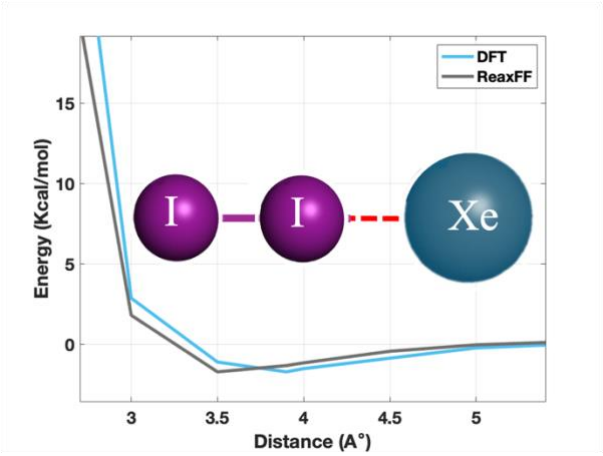

(d) colinear Xe/I_2 interaction

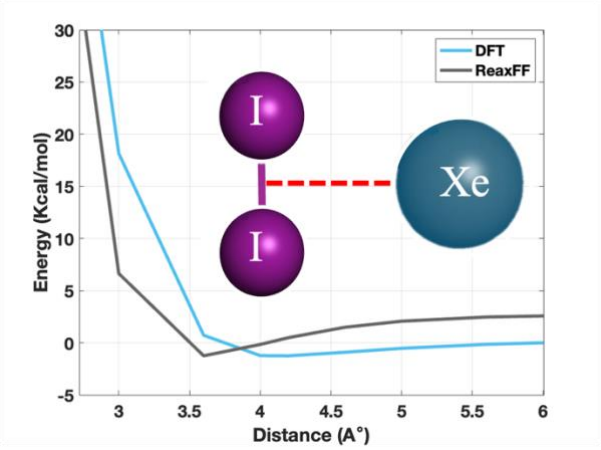

(e) perpendicular Xe/I_2 interaction

Fig.1. Energy calculated from DFT (Blue), ReaxFF (grey), CASSCF (yellow), CCSD (green) and Lennard-Jones (Purple) for (a) Xe/Xe, (b) I/I, (c) Xe/I, (d) colinear Xe/I2, and (e) perpendicular Xe/I2 pairs interactions.

Initial ReaxFF-MD simulations revealed the formation of I_3 molecules with a cyclic structure, particularly under high-pressure conditions or when simulations extended beyond a time scale of 1 nanosecond. The appearance of I_3 molecules in these simulations is non-physical, since this molecule, typically with a linear configuration in its natural state, is energetically unfavorable compared to I_2. Thus, DFT bond scan simulations were performed to study the energy level and to be added to the training set for force field training. DFT simulations were performed using the GGA:PBE DFT functional [45] and TZP basis set, which were implemented in ADF/AMS software [46]. Using the energy values of the DFT diagram and performing a single-parameter search optimization, the force field parameters of the I-I-I angle are trained. The result of the ReaxFF-MD bond scan simulation compared with DFT are shown in figure 2a and figure 2b before and after training the force field. The I_3 cyclic molecule was initially too stable, with exhibiting lower energy compared to I_2 molecule, in the ReaxFF-MD simulation before training the force field (figure 2a), while the result of the Trained force field shows a significantly improved description of the I_3 molecule and its cyclization (figure 2b).

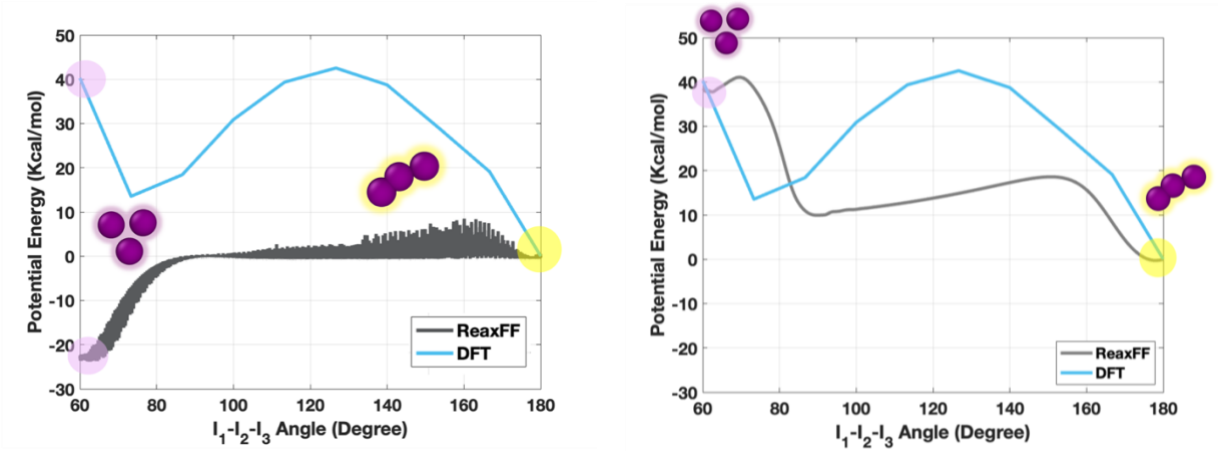

(a) Before training the force field

(b) After training the force field

Fig.2. Energy calculated from ReaxFF-MD and DFT bond scan simulations.

The ReaxFF energy descriptions are in good agreement with the QM data, demonstrating the force field's ability to accurately describe the dynamics of xenon atoms and the recombination of iodine atoms. Force field parameters are given in the supporting information.

3.2.Liquid-like to gas-like state transition (cluster size distribution and size effect)

The embedded molecular clusters among unbound molecules would cause local density inhomogeneities. Thus, we can define a cluster as a group of fluid molecules or atoms that increases the local density of the fluid [3]. There are different ways to define clusters using energetic or geometric criteria [48], [49]. In the present study DBSCAN is used, which assigns all atoms or molecules within a specific distance to the same cluster. We considered the distance to be $5.084 A^{\circ}$ which represents the location of the first peak in the radial distribution function (RDF). The minimum points (MinPts) parameter for the DBSCAN method were set 4 in this study. Moreover, the Hill method [48] (energetic criteria) cluster definition and its comparison with DBSCAN method (geometric criteria) is presented in supplementary information for gas-like, supercritical and liquid-like state which shows that these methods are comparable (see Supplementary Figure 1).

To ensure of the accuracy of our force field, before studying the dynamics of Xenon solvent and its effect on Iodine recombination, we performed ReaxFF-MD simulations for a system consisting of 11000 Xenon atoms at a temperature of 320K and compared the clustering behavior predicted by the ReaxFF method with Lennard-Jones potential which reported by Yoshii and Okazaki [49]. The results of these simulations are reported in Table 1 for different densities. The results demonstrate that increasing the density, and consequently the pressure, leads to the formation of larger clusters. In the first case, the majority of the atoms contribute to a single large cluster consisting of 6733 atoms. In contrast, the second and third cases exhibit a higher number of smaller clusters, predominantly with sizes of 10 and 4 atoms, respectively. The literature has also illustrated the structure of clusters with three and four atoms which we were able to confirm. The average number of each cluster size during the simulation using DBSCAN method and their structures obtained from OVITO for the system with density of 0.055 g/cm^3 are presented in figure 3.

Table 1. Simulation Conditions and Largest Xenon Cluster Sizes: Current Study vs. Literature

	Current Study			Literature [49]
	First case	Second case	Third case	
# of Atoms	11000	11000	11000	10976
Temperature (K)	320	320	320	290-320

Density (gram/cm^3)	8.2122	0.51407	0.05516	0.055-2.7
Largest Cluster Size	6733	10	4	Up to 500

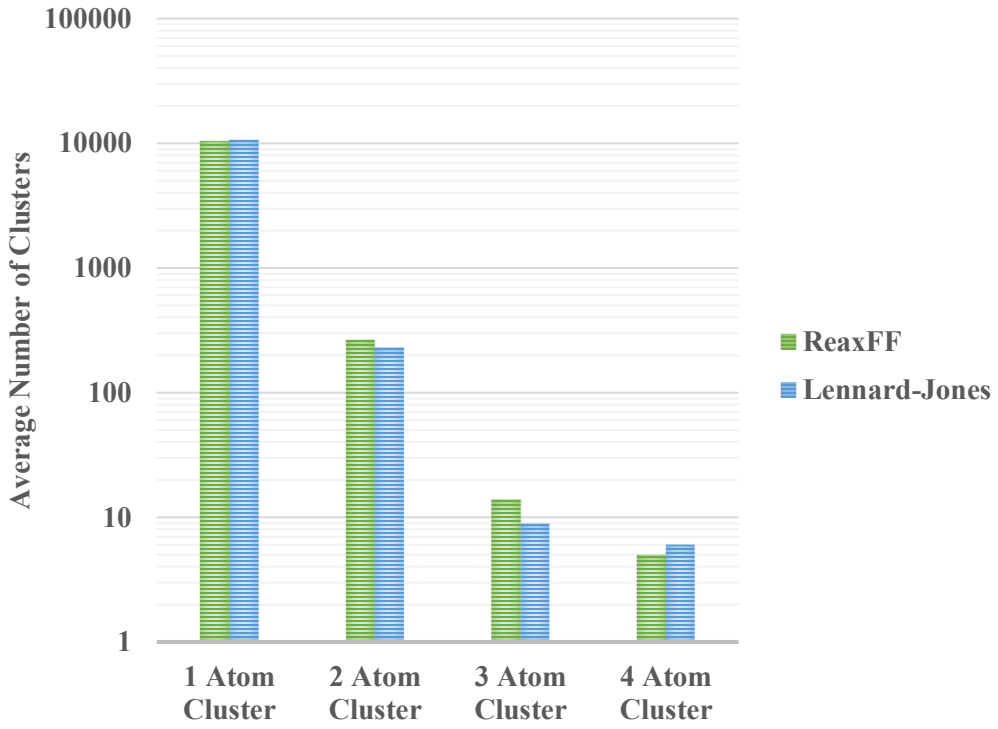

(a)

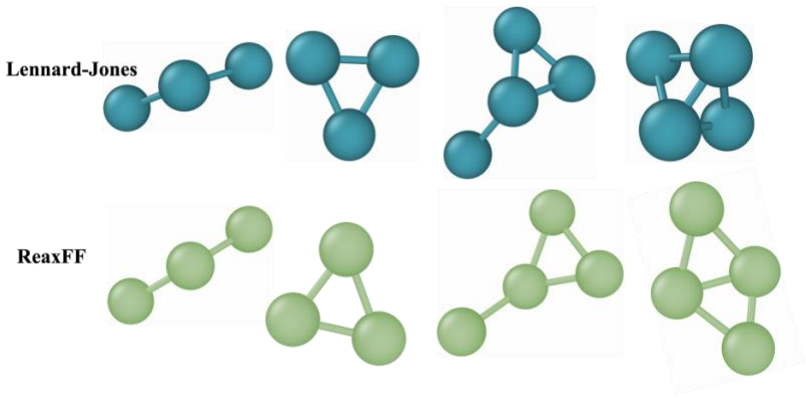

(b)

Fig.3. ReaxFF accuracy compared to Lennard-Jones potential for the system with a density of 0.05516 g/cm^3. (a) Average number of clusters with specific size diagram, (b) Structures of clusters with size three and four from Lennard-Jones force field (Blue clusters) and ReaxFF forcefield (Green clusters) MD simulations.

To study the system size effect on the cluster size distribution and reducing the effect of the finite size of the simulations on the clusters, various systems were modeled with 500, 1000, 4000, and

10000 Xenon atoms, all maintained at a temperature of 290 K and a pressure of 58.98 bar. An examination of the cluster size distribution for these systems, as illustrated in figure 4, reveals a subtle increased occurrence of clusters at a consistent size and the formation of somewhat larger clusters by increasing the size of the system. This suggests that systems with size range of 1000 atoms to 10000 atoms are behaving quite similar in the formation of clusters and we can use smaller system with size of 1000 atoms to reduce the computational cost.

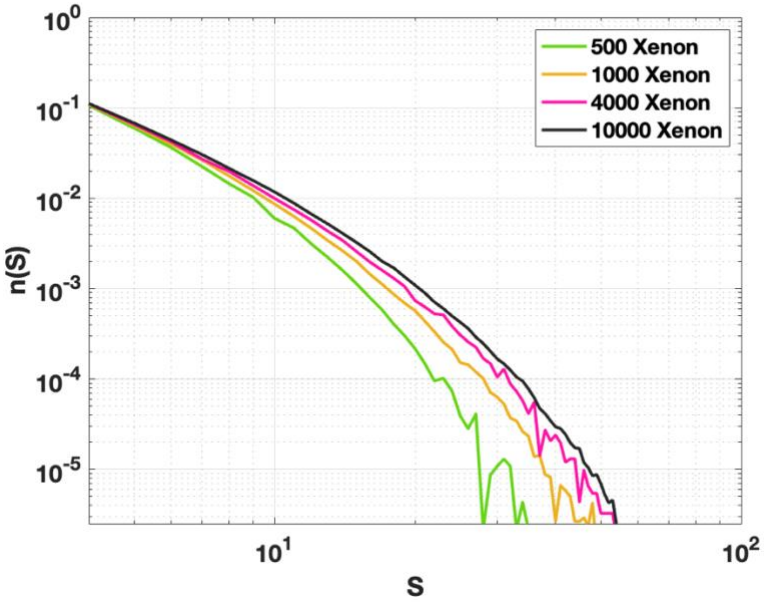

Fig.4. Cluster size distribution for different systems at a temperature of 290 K and a pressure of 58.98 bar

To understand the behavior of the Xenon system at different thermodynamic state conditions, simulations with different temperatures in the range of 202.6- 636.6K and the same pressure of 58.98 bar were performed. The properties of the supercritical Xenon system change when crossing the Widom line. The Widom line is determined as the locus of the maxima of different thermodynamic response functions, originating from the critical point. The slope of this line used for the Xenon system in our study was obtained from NIST [50].

Figure 5 presents the cluster size distribution as well as the largest cluster for different temperatures of an isobaric condition which is the transition from liquid-like state to gas-like state. Figure 5a clearly shows the formation of larger clusters in the liquid-like state, and as we move toward the gas-like state, the largest cluster size decreases [3]. It is worth mentioning that while the largest

cluster belongs to the liquid-like state, due to its high density, most atoms belong to the largest cluster (explaining the liquid-like state).
Figure 5b, where 's' represents the number of atoms in a cluster, and 'n(s)' represents the probability density of cluster of size 's', shows that at subcritical temperature conditions (liquid-like state), atoms contribute more toward the formation of clusters and most atoms belong to a single large cluster. As the temperature increases and the system reaches a supercritical state, the large cluster fragments into several clusters of different sizes. If the temperature is increased beyond the critical point, causing the system to transition to a gas-like state, only a few clusters will remain.
To obtain a large number of clusters in a system with a reasonably large size, the Widom line would be the optimal condition.

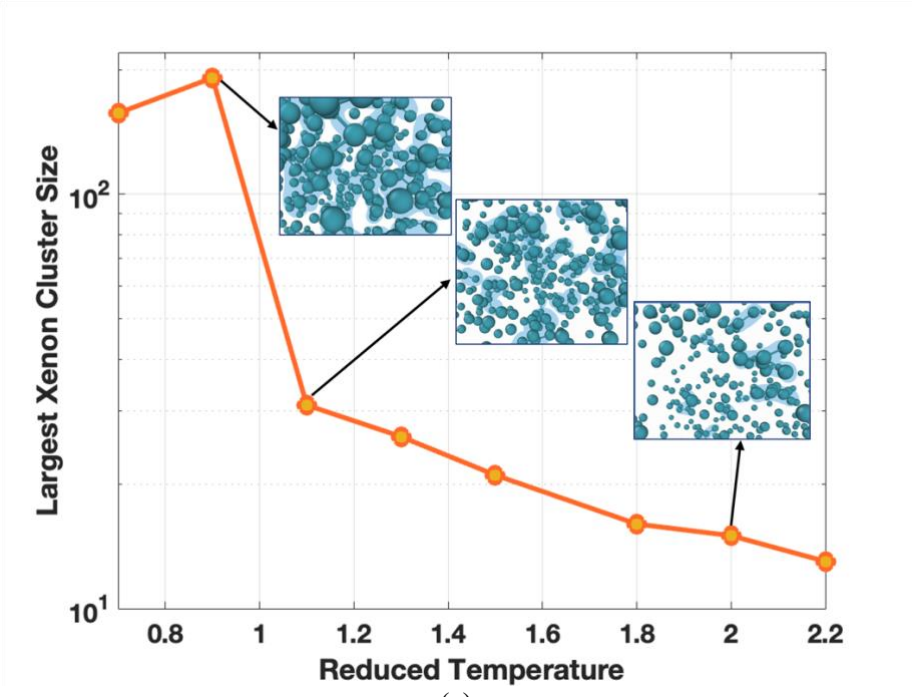

(a)

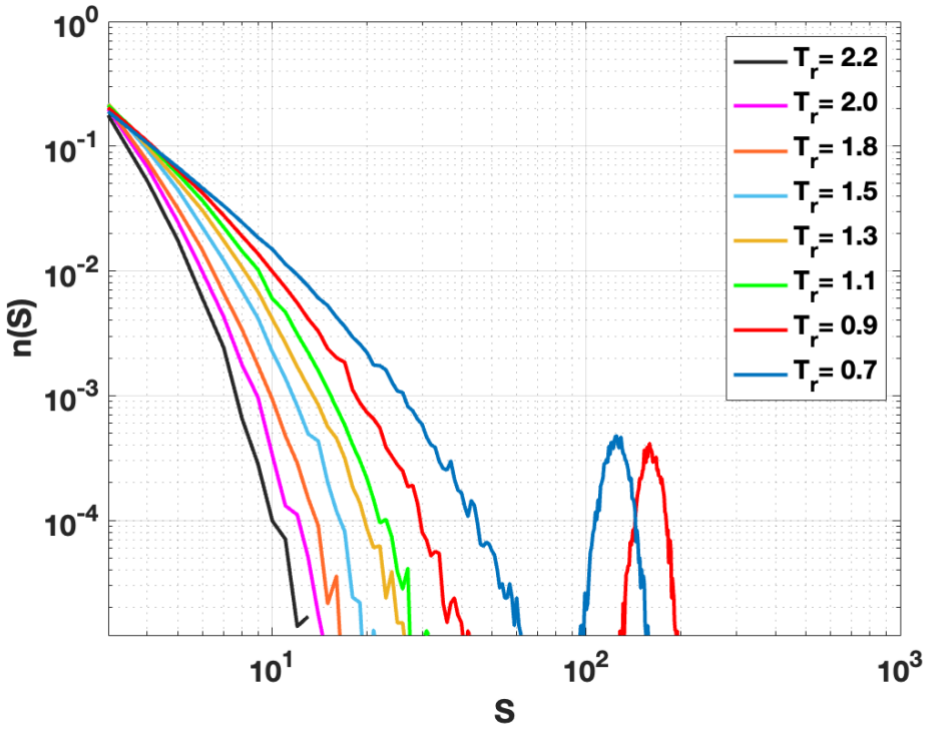

(b)

Fig.5. Liquid-like gas-like state transition for a system containing 1000 Xenon atoms
a) Largest cluster size, b) number of clusters with specific size, at different Temperature conditions at pressure of 58.98 bar crossing the Widom line. The snapshots show the clustering in MD simulation at different temperature conditions. Xenon atoms are represented in dark green, and clusters are shaded in light green.

To investigate changes in the fluid behavior for different thermodynamic conditions along the Widom line, we performed ReaxFF-MD simulations for different supercritical conditions. In figure 6, the cluster size distribution diagram for a system comprising 1000 Xenon atoms is displayed for each condition depicted inset. This diagram shows that the system behaves more like a liquid as it moves away from the critical condition.

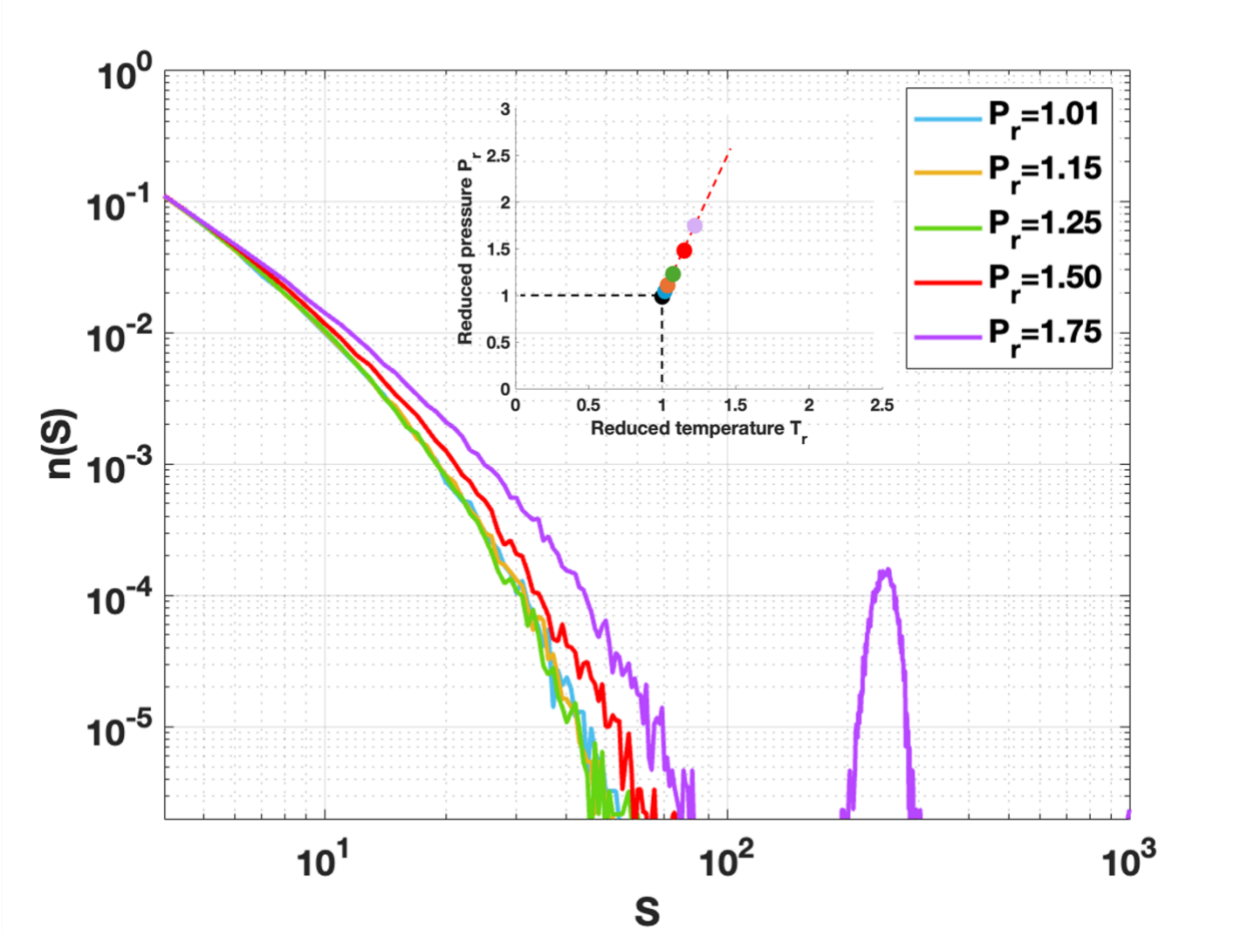

Fig.6. Cluster size distribution at Widom line for a system with 1000 Xenon atoms. The black point is the critical point with a temperature of 289.39K and a pressure of 58.39 bar. Blue, orange, green, red, and purple points on the Widom line (red dashed line) each represent reduced pressure of 1.01, 1.15, 1.25, 1.5, and 1.75, respectively.

3.3. Clusters lifetime

Examining the lifetime of Xenon clusters is crucial, prior to delving into analysis of Iodine recombination within the Xenon system at supercritical conditions. Clusters with lifetime comparable to Iodine recombination timescales can influence the reaction kinetics through caging effect. The cluster's lifetime has been defined as the duration between its formation and the point at which it loses half of its initial atoms. The average lifetime of each cluster is illustrated in figure 7 for a system consisting of 1000 atoms at a temperature of 290 K and different pressures. The initial observation indicates that the size of a cluster and its lifetime are positively correlated, which is consistent with findings reported by Yoshii et al. [49]. Furthermore, given the expected rapid

formation of Iodine molecules (0.6-10 ps [51], [52]), it appears that the average lifetime of Xenon clusters in ranges between 5-11 ps is sufficient to accommodate Iodine atoms within them prior to recombination.

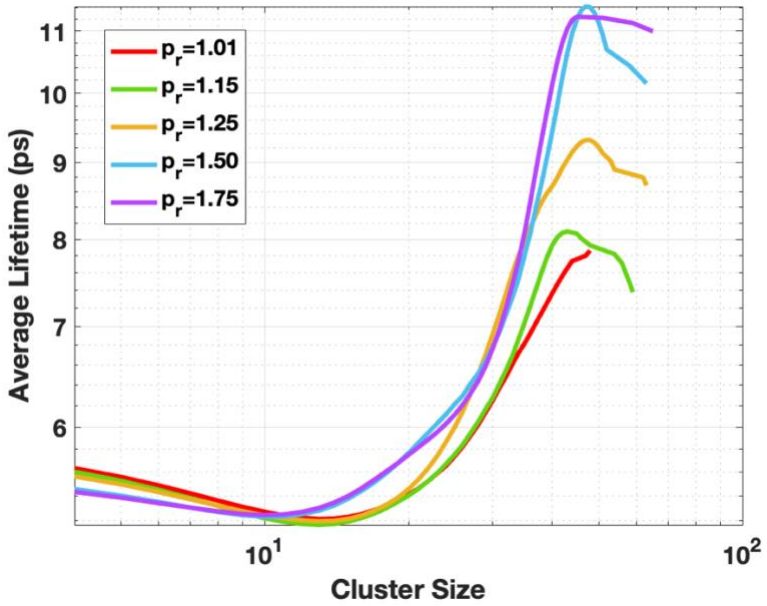

Fig.7. Average lifetime of clusters for a system consists of 1000 Xenon atoms at a temperature of 290 K

3.4.Iodine recombination

To study the Iodine recombination in Xenon solvent using ReaxFF-MD simulations, a system consisting of 10000 Xenon and 250 Iodine atoms was modeled at a temperature of 290 K and a pressure of 58.98 bar employing different ensembles (single thermostat NVT with temperature damping of 1000 fs, Multiple thermostat NVT with temperature damping of 1000 fs for Xenon atoms and temperature damping of 1000000 fs for Iodine atoms, and NVE), with a timestep of 0.25 fs for 1 nanosecond (ns).

The number of Iodine molecules has been tracked, as well as the potential energy and the temperature of the system in figure 8. The solid lines in this diagram are the average value for ten runs with random starting configurations and translucent area in temperature and potential energy curves indicates the error band. In experimental conditions, the system is maintained at a given temperature due to the small number of Iodine atoms added to the Xenon system and this can be

achieved via thermostats in the MD simulations. Therefore, NVE simulations which cannot accurately mimic the supercritical condition of solvent with a linear temperature increase, is not a good choice in Iodine recombination simulations. Within 1 nanosecond, 98 Iodine molecules were formed within a nanosecond using multiple thermostats, and with the formation of each Iodine molecule, there was a rise in temperature and a decrease in potential energy. However, employing a single thermostat NVT, there are 92 Iodine molecules at the end of the simulation, owing to the stronger damping parameter on Iodine atoms which prevent their recombination. Thus, the Temperature fluctuations caused by Iodine molecule formation for a simulation with multiple thermostats are more evident than in a single thermostat case (Figure 8b).

The multiple thermostat NVT ensemble was implemented in the following simulations to study Iodine recombination.

These simulations indicate that the Xenon clusters effectively increase the probability of the formation of Iodine molecules since Iodine atoms without a solvent to transfer excess energy can hardly make a permanent I-I bond.

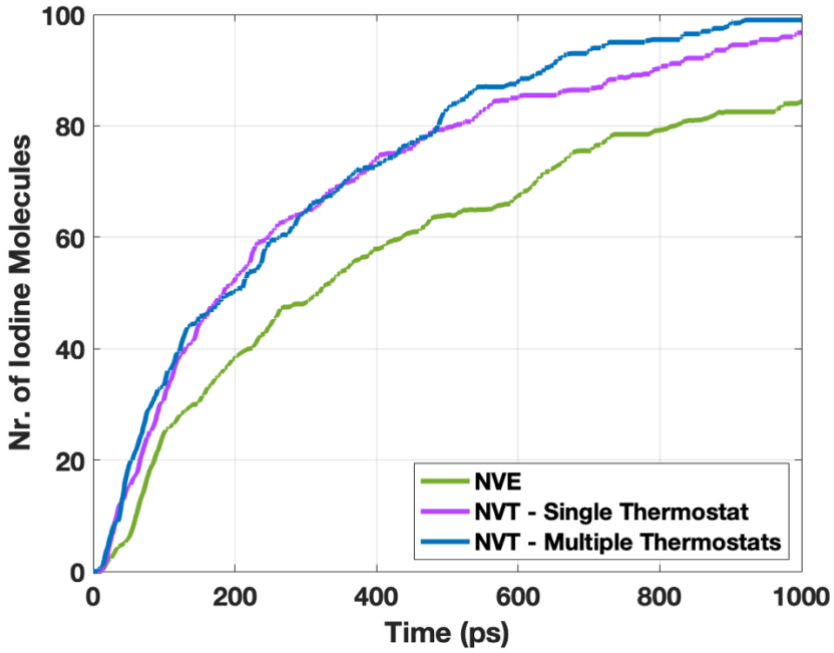

(a)

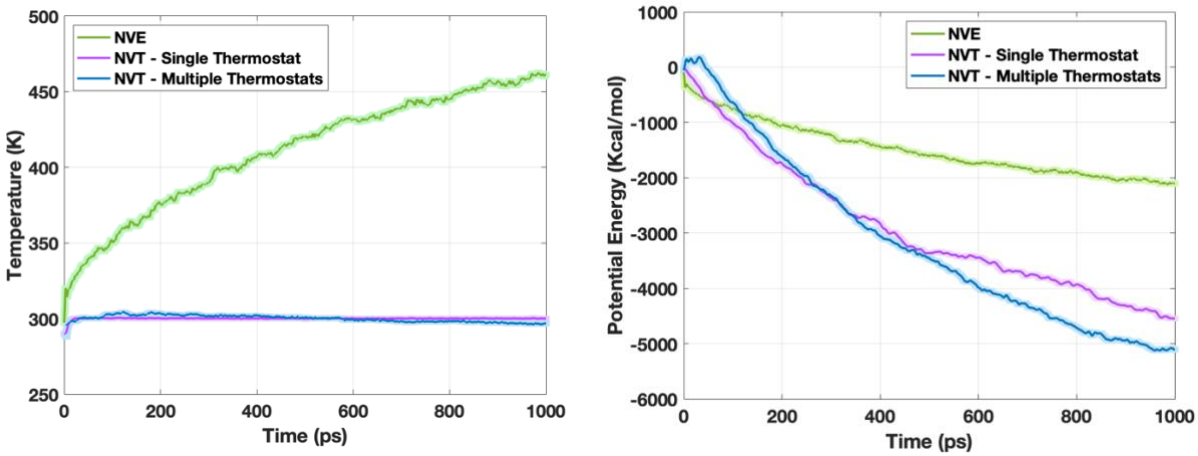

(b) (c)

Fig. 8. a) Formation of Iodine molecules and b) temperature and c) Potential energy change for a system of 10000Xenon and 250 Iodine atoms at a temperature of 290 K and a pressure of 58.98 bar

To gain further insight into the effect of thermodynamic condition on Iodine recombination, the impact of the system's density on the recombination rate constant was investigated. To increase the recombination probabilities, the system with 10000 Xenon atoms and 250 Iodine atoms modeled at a temperature of 290 K and different densities of 10^{-4}, 5×10^{-4}, 10^{-3}, 5×10^{-3}, 10^{-2}, 2×10^{-2} mol/cm^3.

The second-order rate constant can be obtained by calculating the concentration of free Iodine atoms and Iodine molecules at each timestep [18].

$$K = \frac{1}{[I]^2}.\frac{d[I_2]}{dt} \qquad \text{Equation 3}$$

The diagram in figure 9 illustrates the recombination rate constant at different densities. An increase in density increases the effective collision of Iodine atoms by increasing the pressure, resulting in higher Iodine recombination per timestep. The departure from linearity in this diagram is due to an increase in density where the rate limiting process is diffusion. The highlighted part of the curve is where the system is at supercritical condition and provides the highest recombination rate constant.

We have examined the recombination rate constant for this system with a density of 10^{-3} mol/cm^3 over longer timescales, specifically 1.5,2,3,4,5,6 nanoseconds. The recombination rate of Iodine is initially higher according to geminate recombination of Iodine atoms within Xenon clusters, but this would later converge since after that there would be only diffusive recombination (Figure 9b).

Thus, Extending the simulation time to these longer timescales aims to bring our results closer to experimental findings.

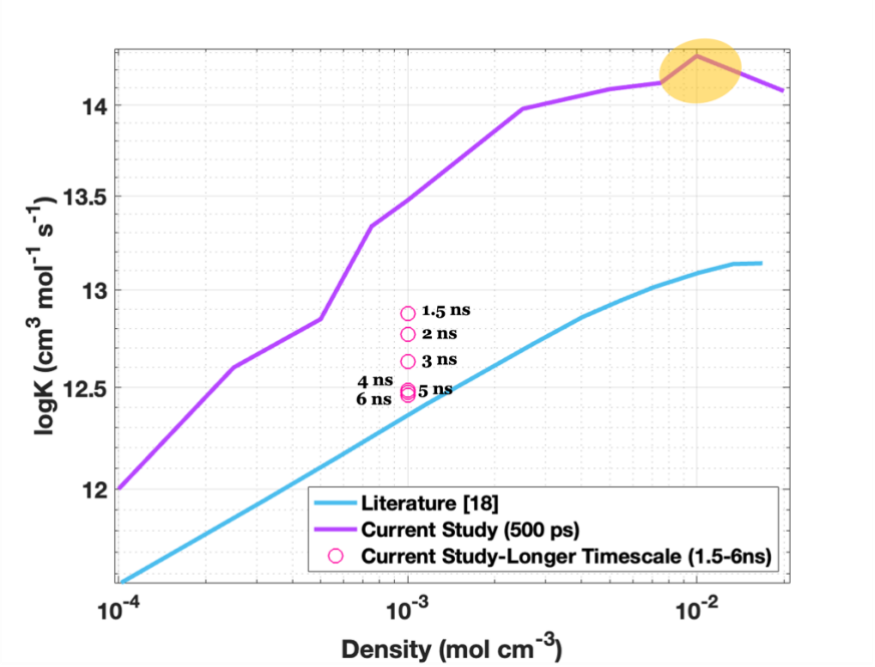

(a)

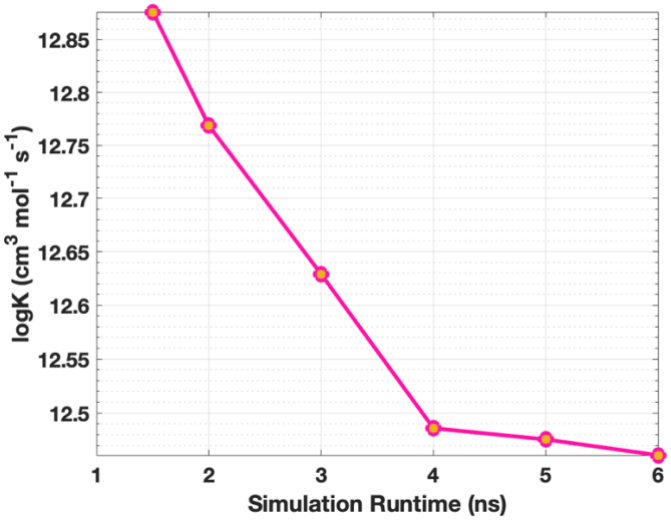

(b)

Fig. 9. Recombination rate constant (a) at different densities over 500 ps and (b) at density of 10^{-3} mol/cm^3 over simulation time ranging from 500 ps to 6 ns

Conclusion

In this study, we performed ReaxFF reactive force field MD simulations to investigate the dynamics of Xenon solvent under different state conditions, as well as to determine the highest rate of Iodine recombination reaction in this solvent.

We developed Xe/I force field parameters against a set of data obtained from DFT calculations so that the developed force field can reproduce the dissociation energies of each atomic pair well. Further validation is accomplished via cluster size and structure analysis, showing good agreement with a Lennard-Jones MD simulation study.

Cluster size distribution analysis for Xenon solvent shows that the supercritical condition, significantly closer to the critical condition, with large number of reasonably large size clusters, is the best thermodynamic condition to study the cage effect. Our findings reveal Xenon clusters as a favorable environment for accommodating Iodine atoms prior to recombination due to clusters' lifetime in ranges of 5-11 ps. Importantly, our findings highlight the significant impact of Xenon solvent on the recombination kinetics of Iodine, showing higher recombination rates in systems with higher density, with the effect being pronounced in the supercritical condition. Beyond supercritical condition, with the high pressure condition where the diffusion is the rate limiter, the recombination rate decreases.

This comprehensive investigation not only enhances our understanding on how solvents influence recombination processes but also provides valuable insights into the design of effective reaction environments for more complex chemical reactions.

Acknowledgment

Reference

[1] G. G. Simeoni *et al.*, 'The Widom line as the crossover between liquid-like and gas-like behaviour in supercritical fluids', *Nat Phys*, vol. 6, no. 7, pp. 503–507, 2010, doi: 10.1038/nphys1683.

[2] P. A. Hoijemberg, J. Zerbs, M. L. Japas, C. A. Chesta, J. Schroeder, and P. F. Aramendía, 'Cage Effect in Supercritical Fluids and Compressed Gases in the Photolysis of an Asymmetrically Substituted Diazene', *J Phys Chem A*, vol. 113, no. 18, pp. 5289–5295, May 2009, doi: 10.1021/jp811390m.

[3] F. Simeski and M. Ihme, 'Supercritical fluids behave as complex networks', *Nat Commun*, vol. 14, no. 1, p. 1996, 2023, doi: 10.1038/s41467-023-37645-z.

[4] G. Brunner, 'Applications of Supercritical Fluids', *Annu Rev Chem Biomol Eng*, vol. 1, no. 1, pp. 321–342, Jun. 2010, doi: 10.1146/annurev-chembioeng-073009-101311.

[5] Y. Zhao, L. Sun, X. Yu, and W. Sun, 'Supercritical Xe as Propellant in Satellite Electric Propulsion System: Experimental Study on Thermal Physical Properties', *IOP Conf Ser Mater Sci Eng*, vol. 562, no. 1, p. 012086, 2019, doi: 10.1088/1757-899X/562/1/012086.

[6] M. OSCHWALD* *et al.*, 'INJECTION OF FLUIDS INTO SUPERCRITICAL ENVIRONMENTS', *Combustion Science and Technology*, vol. 178, no. 1–3, pp. 49–100, Jan. 2006, doi: 10.1080/00102200500292464.

[7] I. Khudyakov, 'Cage Effect', Feb. 2019.

[8] Z. Qiu and C. N. Neumann, 'Influence of Cage Effects in Directing the Outcome of C–X Bond Forming Reactions', *ACS Organic & Inorganic Au*, vol. 4, no. 1, pp. 1–25, Feb. 2024, doi: 10.1021/acsorginorgau.3c00044.

[9] J. Franck and E. Rabinowitsch, 'Some remarks about free radicals and the photochemistry of solutions', *Transactions of the Faraday Society*, vol. 30, pp. 120–130, 1934, doi: 10.1039/tf9343000120.

[10] Zimmerman J. ; Noyes R.M., '.', *J. Chem. Phys*, vol. 18, 1950.

[11] D. Booth and R. M. Noyes, 'The Effect of Viscosity on the Quantum Yield for Iodine Dissociation', *J Am Chem Soc*, vol. 82, no. 8, pp. 1868–1872, 1960, doi: 10.1021/ja01493a009.

[12] H. Hippler, K. Luther, and J. Troe, 'Recombination of iodine atoms in gases at high pressures', *Chem Phys Lett*, vol. 16, no. 1, pp. 174–176, 1972, doi: https://doi.org/10.1016/0009-2614(72)80484-6.

[13] K. Luther and J. Troe, 'Photolytic cage effect of iodine in gases at high pressures', *Chem Phys Lett*, vol. 24, no. 1, pp. 85–87, 1974, doi: 10.1016/0009-2614(74)80220-4.

[14] J.-C. Dutoit, J.-M. Zellweger, and H. Van Den Bergh, 'The photolytic cage effect of iodine in gases and liquids', *J Chem Phys*, vol. 78, no. 4, pp. 1825–1837, 1983, doi: 10.1063/1.444979.

[15] B. Otto, J. Schroeder, and J. Troe, 'Photolytic cage effect and atom recombination of iodine in compressed gases and liquids: Experiments and simple models', *J Chem Phys*, vol. 81, no. 1, pp. 202–213, Jul. 1984, doi: 10.1063/1.447363.

[16] M. G. Sceats, J. M. Dawes, and D. P. Millar, 'Atom recombination in dense gases and fluids—a stochastic model', *Chem Phys Lett*, vol. 114, no. 1, pp. 63–70, 1985, doi: https://doi.org/10.1016/0009-2614(85)85056-9.

[17] T. J. Chuang, G. W. Hoffman, and K. B. Eisenthal, 'Picosecond studies of the cage effect and collision induced predissociation of iodine in liquids', *Chem Phys Lett*, vol. 25, no. 2, pp. 201–205, 1974, doi: https://doi.org/10.1016/0009-2614(74)89117-7.

[18] J. -C. Dutoit, J. -M. Zellweger, and H. van den Bergh, 'The photolytic cage effect of iodine in gases and liquids', *J Chem Phys*, vol. 78, no. 4, pp. 1825–1837, Feb. 1983, doi: 10.1063/1.444979.

[19] V. J. Krukonis, M. A. McHugh, and A. J. Seckner, 'Xenon as a supercritical solvent', *J Phys Chem*, vol. 88, no. 13, pp. 2687–2689, Jun. 1984, doi: 10.1021/j150657a004.

[20] K. Radan and B. Žemva, 'Solvent capabilities of liquid and supercritical xenon', 2012. [Online]. Available: https://api.semanticscholar.org/CorpusID:14449499

[21] R. K. Upmacis, M. Poliakoff, and J. J. Turner, 'Structure and thermal reactions of dihydrogen complexes: the IR characterization of M(CO)5(H2) (M = chromium, molybdenum, and tungsten) and cis-Cr(CO)4(H2)2 in liquid xenon solution and the formation of HD during exchange of hydrogen and deuterium', *J Am Chem Soc*, vol. 108, pp. 3645–3651, 1986, [Online]. Available: https://api.semanticscholar.org/CorpusID:101951034

[22] M. B. Sponsler, B. H. Weiller, P. O. Stoutland, and R. G. Bergman, 'Liquid xenon: an effective inert solvent for carbon-hydrogen oxidative addition reactions', *J Am Chem Soc*, vol. 111, no. 17, pp. 6841–6843, Aug. 1989, doi: 10.1021/ja00199a054.

[23] D. L. Bunker and B. S. Jacobson, 'Photolytic Cage Effect. Monte Carlo Experiments', *J Am Chem Soc*, vol. 94, no. 6, pp. 1843–1848, 1972, doi: 10.1021/ja00761a009.

[24] A. J. Stace and J. N. Murrell, 'Molecular dynamics and chemical reactivity', *Mol Phys*, vol. 33, no. 1, pp. 1–24, Jan. 1977, doi: 10.1080/00268977700103001.

[25] J. T. Hynes, R. Kapral, and G. M. Torrie, 'Stochastic trajectory simulation of iodine recombination in liquids', *J Chem Phys*, vol. 72, no. 1, pp. 177–188, Jul. 2008, doi: 10.1063/1.438961.

[26] M. F. Russo and A. C. T. van Duin, 'Atomistic-scale simulations of chemical reactions: Bridging from quantum chemistry to engineering', *Nucl Instrum Methods Phys Res B*, vol. 269, no. 14, pp. 1549–1554, 2011, doi: https://doi.org/10.1016/j.nimb.2010.12.053.

[27] K. Chenoweth, A. C. T. van Duin, P. Persson, M.-J. Cheng, J. Oxgaard, and W. A. I. I. I. Goddard, 'Development and Application of a ReaxFF Reactive Force Field for Oxidative Dehydrogenation on Vanadium Oxide Catalysts', *The Journal of Physical Chemistry C*, vol. 112, no. 37, pp. 14645–14654, Sep. 2008, doi: 10.1021/jp802134x.

[28] M. F. Russo, R. Li, M. Mench, and A. C. T. van Duin, 'Molecular dynamic simulation of aluminum–water reactions using the ReaxFF reactive force field', *Int J Hydrogen Energy*, vol. 36, no. 10, pp. 5828–5835, 2011, doi: https://doi.org/10.1016/j.ijhydene.2011.02.035.

[29] K. Chenoweth, A. C. T. van Duin, and W. A. Goddard, 'ReaxFF Reactive Force Field for Molecular Dynamics Simulations of Hydrocarbon Oxidation', *J Phys Chem A*, vol. 112, no. 5, pp. 1040–1053, Feb. 2008, doi: 10.1021/jp709896w.

[30] T. P. Senftle *et al.*, 'The ReaxFF reactive force-field: development, applications and future directions', *NPJ Comput Mater*, vol. 2, no. 1, p. 15011, 2016, doi: 10.1038/npjcompumats.2015.11.

[31] A. D. Jr. MacKerell *et al.*, 'All-Atom Empirical Potential for Molecular Modeling and Dynamics Studies of Proteins', *J Phys Chem B*, vol. 102, no. 18, pp. 3586–3616, Apr. 1998, doi: 10.1021/jp973084f.

[32] W. L. Jorgensen, D. S. Maxwell, and J. Tirado-Rives, 'Development and Testing of the OPLS All-Atom Force Field on Conformational Energetics and Properties of Organic Liquids', *J Am Chem Soc*, vol. 118, no. 45, pp. 11225–11236, Nov. 1996, doi: 10.1021/ja9621760.

[33] B. H. Morrow and J. A. Harrison, 'Evaluating the Ability of Selected Force Fields to Simulate Hydrocarbons as a Function of Temperature and Pressure Using Molecular Dynamics', *Energy & Fuels*, vol. 35, no. 5, pp. 3742–3752, Mar. 2021, doi: 10.1021/acs.energyfuels.0c03363.

[34] J. O. Hirschfelder, C. F. Curtiss, and R. B. Bird, *The Molecular Theory of Gases and Liquids*. in Molecular Theory of Gases and Liquids. Wiley, 1954. [Online]. Available: https://books.google.com/books?id=BJkuAAAAIAAJ

[35] K. Vanommeslaeghe *et al.*, 'CHARMM general force field: A force field for drug-like molecules compatible with the CHARMM all-atom additive biological force fields', *J Comput Chem*, vol. 31, no. 4, pp. 671–690, Mar. 2010, doi: https://doi.org/10.1002/jcc.21367.

[36] J. Fischer and M. Wendland, 'On the history of key empirical intermolecular potentials', *Fluid Phase Equilib*, vol. 573, p. 113876, 2023, doi: https://doi.org/10.1016/j.fluid.2023.113876.

[37] J. P. Perdew, K. Burke, and M. Ernzerhof, 'Generalized Gradient Approximation Made Simple', *Phys Rev Lett*, vol. 77, no. 18, pp. 3865–3868, Oct. 1996, doi: 10.1103/PhysRevLett.77.3865.

[38] F. Weigend, 'Accurate Coulomb-fitting basis sets for H to Rn', *Physical Chemistry Chemical Physics*, vol. 8, no. 9, pp. 1057–1065, 2006, doi: 10.1039/B515623H.

[39] S. Grimme, 'Semiempirical GGA-type density functional constructed with a long-range dispersion correction', *J Comput Chem*, vol. 27, no. 15, pp. 1787–1799, Nov. 2006, doi: https://doi.org/10.1002/jcc.20495.

[40] N. Godbout, D. R. Salahub, J. Andzelm, and E. Wimmer, 'Optimization of Gaussian-type basis sets for local spin density functional calculations. Part I. Boron through neon, optimization technique and validation', *Can J Chem*, vol. 70, no. 2, pp. 560–571, Feb. 1992, doi: 10.1139/v92-079.

[41] C. Sosa, J. Andzelm, B. C. Elkin, E. Wimmer, K. D. Dobbs, and D. A. Dixon, 'A local density functional study of the structure and vibrational frequencies of molecular transition-metal compounds', *J Phys Chem*, vol. 96, no. 16, pp. 6630–6636, Aug. 1992, doi: 10.1021/j100195a022.

[42] B. O. Roos, 'The Complete Active Space Self-Consistent Field Method and its Applications in Electronic Structure Calculations', in *Advances in Chemical Physics*, in Advances in Chemical Physics. , 1987, pp. 399–445. doi: https://doi.org/10.1002/9780470142943.ch7.

[43] R. Guo and K. Balasubramanian, 'Spectroscopic properties and potential energy curves of low-lying electronic states of RuC', *J Chem Phys*, vol. 120, no. 16, pp. 7418–7425, Apr. 2004, doi: 10.1063/1.1688755.

[44] M. J. ea Frisch *et al.*, 'Gaussian 16', 2016, *Gaussian, Inc. Wallingford, CT*.

[45] A. M. Ritzmann, M. D. LaCount, M. Sassi, A. E. Johnson, and N. J. Henson, 'A density functional theory analysis of the adsorption and surface chemistry of inorganic iodine species on graphitea', *Frontiers in Nuclear Engineering*, vol. 2, 2023, [Online]. Available: https://www.frontiersin.org/articles/10.3389/fnuen.2023.1170424

[46] G. te Velde *et al.*, 'Chemistry with ADF', *J Comput Chem*, vol. 22, no. 9, pp. 931–967, Jul. 2001, doi: https://doi.org/10.1002/jcc.1056.

[47] A. C. T. van Duin, J. M. A. Baas, and B. van de Graaf, 'Delft molecular mechanics: a new approach to hydrocarbon force fields. Inclusion of a geometry-dependent charge calculation', *Journal of the Chemical Society, Faraday Transactions*, vol. 90, no. 19, pp. 2881–2895, 1994, doi: 10.1039/FT9949002881.

[48] T. L. Hill, 'Molecular Clusters in Imperfect Gases', *J Chem Phys*, vol. 23, no. 4, pp. 617–622, Dec. 2004, doi: 10.1063/1.1742067.

[49] N. Yoshii and S. Okazaki, 'A large-scale and long-time molecular dynamics study of supercritical Lennard-Jones fluid. An analysis of high temperature clusters', *J Chem Phys*, vol. 107, no. 6, pp. 2020–2033, Aug. 1997, doi: 10.1063/1.474553.

[50] P. Linstrom and W. Mallard, 'The NIST Chemistry WebBook: A Chemical Data Resource on the Internet', 2001.

[51] Q. Liu, J.-K. Wang, and A. H. Zewail, 'Femtosecond dynamics of dissociation and recombination in solvent cages', *Nature*, vol. 364, no. 6436, pp. 427–430, 1993, doi: 10.1038/364427a0.

[52] A. L. Harris, J. K. Brown, and C. B. Harris, 'The Nature of Simple Photodissociation Reactions in Liquids on Ultrafast Time Scales', *Annu Rev Phys Chem*, vol. 39, no. Volume 39, pp. 341–366, 1988, doi: https://doi.org/10.1146/annurev.pc.39.100188.002013.